Journal of Materials Chemistry C

Accepted Manuscript

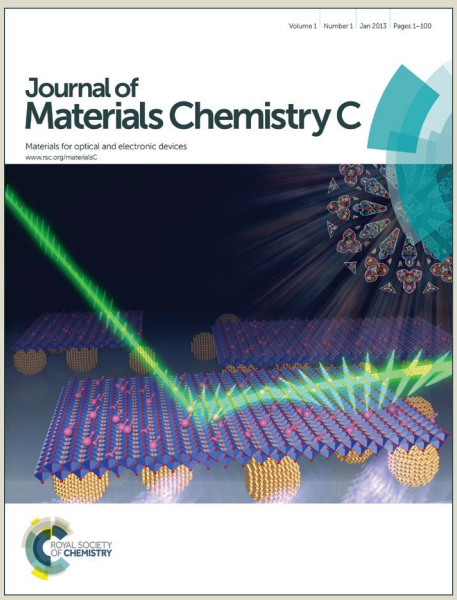

ROYAL SOCIETY OF CHEMISTRY

www.rsc.org/materialsC

Phototransistors based on Donor-Acceptor conjugated polymer with high response speed

Qinghe Wang,[a,b,c] Min Zhu,[a,b,c] Di Wu,[a] Guobing Zhang,[a,b,c] Xiaohong Wang,[a,b,c] Hongbo, Lu,[a,b,c] Xianghua Wang,[a] Longzhen Qiu[a,b,c]*

a. Key Lab of Special Display Technology, Ministry of Education, National Engineering Lab of Special Display Technology, State Key Lab of Advanced Display Technology, Academy of Opto-Electronic Technology, Hefei University of Technology, Hefei, 230009, People's Republic of China.

b. Key Laboratory of Advanced Functional Materials and Devices, Anhui Province, School of Chemistry and Chemical Engineering, Hefei University of Technology, Hefei, 230009, People's Republic of China.

c. School of Chemistry and Chemical Engineering, Hefei University of Technology, Hefei, 230009, People's Republic of China.

* Corresponding author. Tel: +86 055162902821.
E-mail address: lzhqiu@hfut.edu.cn (L Qiu)

Abstract

A photoresponsive polymer thin-film transistor based on a donor-acceptor conjugated polymer ambipolar semiconductor (PBIBDF-BT) is proposed in this report. The device exhibited both hole- and electron-carriers transport response to incident light with photoswitching speeds below 14 ms. In addition, the photocurrent/dark-current ratio and the photoresponsivity were 4552 and 108.43 mAW^{-1} for P-type channel, and 1044 and 38.72 mAW^{-1} for N-type channel, respectively. The PBIBDF-BT films exhibit more pronounced sensitivity to red light than previous polymer semiconductor, and the drain current gradually increased with an increase in the illumination intensity, resulting in typical output field-effect transistor characteristics. The influence of mobility of PBIBDF-BT thin films, which were formed via spin coating at different spinning speeds on the OTS/SiO_2/Si substrate, on the phototransistor response to light illumination was further investigated.

Keywords

Polymer thin-film phototransistor; D-A conjugated polymer semiconductor; response speed; mobility

1. Introduction

Semiconducting polymer thin-film transistors (PTFTs) have attracted tremendous attention due to their advantages such as light weight, low cost, mechanical flexibility, solution processability and large area printability.[1-8] The applications of PTFTs include electronic paper,[9] logic circuitry,[10] radio frequency identification cards,[11] chemical and biological sensing,[12] and phototransistors.[6] Phototransistors, which allow for the transduction and conversion of an optical variation into an electrical signal and provide compatibility with digital read-out methods, are one of promising photodetectors.[13] In comparison with conventional photodiodes, phototransistors exhibit high sensitivity and low noise deriving from the internal signal amplification function of the transistor device. Generally, the detecting process of phototransistors is composed of three critical stages: (1) generating charge carriers under light irradiation, (2) transferring charge carriers in the semiconductor films, and (3) collecting charge carriers for signal magnification.[14, 15] The absorption bands of a semiconductor determines its efficiency of carrier generation under incident light and the mobility dictates the efficiency of the carrier transport and collection for signal. Therefore, a polymer semiconductor with broad absorption bands and a high mobility plays a vital role in the realization of developing a high-performance phototransistor. Among the many types of promising polymer semiconductors, the donor-acceptor (D–A) conjugated polymer is particularly attractive in which conjugated electron-rich and electron-deficient units are amalgamated to prepare alternating copolymers in order to optimize the highest occupied molecular orbital (HOMO) and the lowest unoccupied molecular orbital (LOMO) via intramolecular and intermolecular interactions.[16, 17] In one aspect, the D–A strategy is widely utilized in synthetic design of conjugated polymers with broad absorption bands to harvest more incident photons for efficient charge-carrier generation.[17-20] In addition, the coexistence of a π–π stacking effect and the D–A interaction in the structure of a D–A alternating polymer may induce high crystallinity and dense long-range chain-packing phenomena, resulting in superior charge carrier mobility.[21] D–A polymer-based transistors are reported to have hole mobilities exceeding 10 $cm^2V^{-1}s^{-1}$ [22-27] and electron mobilities over 6 $cm^2V^{-1}s^{-1}$.[28-30] The D–A polymer semiconductors composed of broad absorption and high mobility would enhance the

performance of phototransistors. A number of D–A polymer semiconductors, such as PBDT-BBT,[14] PDVT-10,[4] PPhTQ[21] and DPP4T-*co*-BDT,[13] have been developed for high-performance phototransistors. To evaluate the performance of phototransistors, photoresponsivity (R), photosensitivity (photocurrent/dark-current ratio) (P), and photoswitching speed are major parameters of merit. Most recently, the advancement of materials design has led to the achievement of polymer-based phototransistor with R over 10^3 A W^{-1} and P up to 10^5, which exceed those of Si-based phototransistors (R ≈ 300 A/W and $I_{on}/I_{off} \approx 10^3$). However, compared with the photocurrent decay times of the order of 10 μs for a phototransistor, the response times of polymer-based phototransistors are generally in the order of magnitude of 0.1 to several seconds. These slow photoswitching speeds present a barrier that impedes their practical application in optical communications and image sensors.[31-33]

Several works have transitioned their focus to the switching speed for polymer phototransistors. Dutta reported that the P3HT-based device showed rise time less than 20 ms.[34] Anthopoulos discovered that the device based blend of MDMO-PPV:$PC_{61}BM$ exhibited the rise time off approximately 16 μs.[35] Nevertheless, there are some disadvantages about the method of blending polymers that include phase separation of blended solutions that destroys the homogeneity of the polymer blend film and the process of forming semiconductor layers is difficult to reproduce and is more complicated than polymer thin-film phototransistors. Thus, it's important to found investigate new polymer thin-film phototransistors which possess shorter rise time (T_r) and fall time (T_f) for response speed to light illumination. The polymer semiconductor materials for phototransistors are still worth further investigation considering their promising results.

(3E,7E)-3,7-bis(2-oxoindolin-3-ylidene)benzo-[1,2-b:4,5-b0]-difuran-2,6(3H,7H)-dione (BIBDF), also known as benzodifurandione-based oligo(*p*-phenylene vinylene) (BDOPV), is a relatively new electron-deficient building block developed by Pei's group.[36] The first polymers of BIBDF with thiophene (PBIBDF-T) and bithiophene (PBIBDF-BT) were reported by Li's group.[37] The PBIBDF-T showed an electron mobility of 10^{-2} $cm^2V^{-1}s^{-1}$ while the PBIBDF-BT is insoluble in any solvent. To resolve the insolubility issue, Pei et al. substituted PBIBDF-BT with a larger branch group and improved the electron and hole

mobility up to 1.74 $cm^2V^{-1}s^{-1}$ and 0.47 $cm^2V^{-1}s^{-1}$, respectively.[38] As alternative, we have independently synthesized a soluble PBIBDF-BT by introducing the solubilizing alkyl chain grafted bithiophene unit as the donor and the BIBDF unit as the acceptor.[39] The low band gap polymer with a low-laying LUMO/HOMO energy (-4.03/-5.55 eV) exhibits efficient ambipolar charge transport with electron and hole mobilities as high as 1.08 and 0.3 $cm^2V^{-1}s^{-1}$, respectively, and with broad absorption occurring in the range of 300–1100 nm. The board absorption is advantageous to harvest more incident photons for efficient charge-carrier generation. These features reveal that PBIBDF-BT is an appropriate semiconductor material for polymer thin-film phototransistors. In this paper, we report a phototransistor based on the PBIBDF-BT semiconductor. In comparison to previous reports of D─A conjugated polymer thin-film phototransistors,[13, 14, 17, 21] the polymer thin-film phototransistor (PTFPT) based on PBIBDF-BT exhibited both a hole and electron carrier transport response to incident light at different intensities and exhibited rise and fall times below 14 ms for hole and electron carriers transport. This study further discusses the influences of different mobilities on the phototransistor response to light illumination.

2. Results and discussion

2.1 Characterization of PBIBDF-BT film

Figure 1a presents the molecular structure of PBIBDF-BT. Details of the synthesis are reported in our previous work.[39] The UV-vis-NIR absorption spectra of PBIBDF-BT in dilute chloroform solution, in thin film, and in thin film annealed at 175 °C are shown in Figure 1c. The PBIBDF-BT film exhibited two absorption bands: band I (600─1100 nm) that is a typical charge transfer absorption from the bithiophene unit to the BIBDF core and band II (300─600 nm) that is attributed to the absorption of the bithiphene donor pair. The absorption peaks of PBIBDF-BT in film showed small red-shift in comparison with those in solution. This suggests that the polymers adopted similar geometry both in solution and in film. The absorption properties of PBIBDF-BT films before and after annealing are almost the same, indicating that the annealing process has little influence on the π-π stacking of molecules in PBIBDF-BT film. The broad absorption of PBIBDF-BT is beneficial to harvest more incident photons for efficient charge-carrier generation.

(insert Figure 1 here)

2.2 Characterization of PBIBDF-BT thin-film phototransistor

The PBIBDF-BT transistors were fabricated in the bottom-gate, top contact configuration as displayed in Figure 1b. Firstly, the devices were fabricated in a glove box and measured under vacuum conditions as ascribed in our previous work.[39] However, the device performance showed negligible change under the illumination of light, as shown in Figure S2. Interestingly, as the fabrication and measuring processes were performed under ambient conditions, the device displayed a distinct photo-response.

(insert Figure 2 here)

Figure 2 illustrates the field-effect characteristics of devices based on PBIBDF-BT films spun at 5000 rpm under dark and light illumination. The devices demonstrated ambipolar characteristics with the max and average hole mobility at 0.20 $cm^2V^{-1}s^{-1}$ and 0.17 ± 0.02 $cm^2V^{-1}s^{-1}$, and the max and average electron mobility at 0.07 $cm^2V^{-1}s^{-1}$ and 0.06 ± 0.02 $cm^2V^{-1}s^{-1}$, respectively. The ambipolar characteristics with hole mobility prior to electron mobility is very different to our previous results.[39] The reason could be attributed to the oxygen doping in the polymer film because the device in this work was fabricated and measured under ambient conditions rather than nitrogen and vacuum conditions of our previous work. Upon contact with oxygen, the LUMO level of polymer decreases resulting in shallow electron traps in the polymer film which decreases electron mobility, and the HOMO level of polymer increase, which would reduce the hole injection barrier from the Au electrode and enhance the hole mobility.

To evaluate the photoresponsitivity of the device, the field-effect characteristics of the devices under light illumination with different intensities were characterized. As shown in Figure 2 (a-d), when the devices were exposed to light, the drain current (I_{DS}) clearly increased compared to the I_{DS} value under dark conditions at the same gate voltage (V_{GS}) in both linear ($V_{DS} < V_{GS} - V_{th}$) and saturation ($V_{DS} > V_{GS} - V_{th}$) regions of transfer

characteristics. It is noted that the increment of I_{DS} under red light (650 nm) illumination at the light intensity of 7.61 $mWcm^{-2}$ (white light) was more substantial than that caused by white light illumination at the approximate light intensity of 7.58 $mWcm^{-2}$ (650 nm), which indicates that the PBIBDF-BT films exhibit pronounced sensitivity to red light. A possible explanation could be ascribed to the higher absorption coefficient in the band from 600 to 1100 nm caused by charge transfer absorption from the dithiophene unit to the BIBDF core, as shown in Figure 1 and Figure S1. The absorption coefficient of PBIBDF-BT solutions in the range from 390 to 600 nm is about 1.8×10^4 $M^{-1}cm^{-1}$, and followed by a rapid increase with the increase of wavelength. The maximum absorption coefficient was 8.6×10^4 $M^{-1}cm^{-1}$ at 825 nm. Obviously, the absorption coefficients in the red light region are much larger than those of other visible lights. Therefore, the devices based PBIBDF-BT are more sensitive to red light. With a further increase in red light (650 nm) intensity to 21.68 $mWcm^{-2}$, the I_{DS} further shifted toward higher level for both electrons and holes-carriers transport.

Photoresponsivity (R) and photocurrent/dark-current ratio (P) are crucial parameters assessing the performance of phototransistors, which are defined by the following equations:

$$\mathbf{R} = \frac{I_i - I_{dark}}{SP_{ill}} \quad (1)$$

$$\mathbf{P} = \frac{I_i - I_{dark}}{I_{dark}} \quad (2)$$

where P_{ill} is the incident illumination intensity while S refers to the area of channel region exposed to illumination, I_i the drain current under illumination, I_{dark} the drain current in the dark.[40, 41] The P and R of devices were calculated from Figure 2c and d using equation 1 and 2, the max P values measured under light illumination at the intensities of 7.58, 7.61, 21.68 $mWcm^{-2}$ are 536, 2514, and 4552 for hole-carriers transport, and are 64, 709, 1044 for electron-carriers transport, respectively. Obviously，the P values are increase with increase in the light intensity, and the P value is the same magnitudes compares with previously reported P values of polymer thin-film phototransistors.[40, 42-44] While the max R values are 28.89, 108.43, and 57.65 mAW^{-1} for hole-carriers transport, and are 2.58, 19.47, 19.51 mAW^{-1} for electron-carriers transport, respectively. These R values are lower than the previously reported values of polymer thin-film phototransistors.[4, 13, 21, 45] A possible reason is that the incident light of 650 nm is at the absorption edge of PBIBDF-BT thin-film which may affect

the efficiency of carrier generation. It can be expected that the R value would be improved by using incident light with longer wavelengths, such as the absorption peak of 840 nm.

Figures 2e and f plot the evolution of I_{DS} under illumination with different intensities at fixed V_{GS} in both P- and N- type channels. Similar to organic field-effect transistors using V_{GS} to control the source-drain current, the light is utilized as an independent variable to control the output of the transistor to test light detection and signal magnification in a single organic device. The changes of transfer and output curves with different light intensities correspond to previously reported PTFPTs.[4, 6, 7, 42, 46, 47] The increment of drain current in the PBIBDF-BT thin film upon illumination was a result of the photo-induced excitons that were subsequently dissociated into electrons and holes under the applied gate voltage. For a P channel device, the photoinduced electrons may be immediately trapped in the bulk and interface regions that makes hole transport dominate.[4, 33, 42, 46, 48] For an N channel device, the situation is reversed. Reminding the observation of the absence of photo-response in the PBIBDF-BT device fabricated and measured in inert conditions such as nitrogen and vacuum, the trap site in the PBIBDF-BT PTFPT should arise from the oxygen doping in the polymer film which results in lower LUMO level and higher HOMO level generating shallow electron and hole trap sites, respectively.

(insert Figure 3 here)

The photoswitching properties of PBIBDF-BT phototransistor were also investigated. Figure 3 displays the current response of PBIBDF-BT phototransistor to an on/off illumination at constant V_{DS} and V_{GS}. The photocurrent sharply increases and is stabilized at an 'On' state upon light irradiation, while it decreases quickly to an 'Off' state when the light was turned off. The on/off current ratios of the device with applied fixed negative drain and gate voltages upon light illumination at light intensities of 7.58 $mWcm^{-2}$ (white light), 7.61 $mWcm^{-2}$ (650 nm), and 21.68 $mWcm^{-2}$ (650 nm) were measured to be average values of 10, 135, and 180, respectively. The on/off current ratios of the device at applied fixed positive drain and gate voltages upon light illumination at light intensities of 7.58 $mWcm^{-2}$ (white light), 7.61 $mWcm^{-2}$ (650 nm), 21.68 $mWcm^{-2}$ (650 nm) were measured to be average values

of 10, 62, and 78, respectively. The increase of on/off current ratios with an increase in light intensity were due to the higher on current generated by intense light which is consistent with the change of transfer and output curves under light illumination. Moreover, Figure 3c and 3d present the time dependent photoresponse of the phototransistors measured by periodically turning on and off the light intensity (21.68 $mWcm^{-2}$) of a light source (650 nm) in our measurement system. The stability of PBIBDF-BT phototransistor is confirmed in 7 on-off cycles, showing excellent stability and reproducible characteristics.

(insert Figure 4 here)

The response speed is a key parameter that determines the capability of a photodetector to follow a fast-varying optical signal, which is important for practical applications in optical communications and image sensors. The time taken for an increase of current from 10% to 90% of its peak value or *vice versa* is defined as the rise time and fall time, respectively. Figures 4a and b display the rise time and fall time with hole- and electron-carriers transport of devices. We have observed fast response speed with rise time and fall time that are exceptionally quick at 14 ms and below. However, we could not measure the response speed at shorter times due to limitations of our setup instrumentation. The response speed of PBIBDF-T thin-film phototransistor is faster to light illumination relative to previously reported polymer thin-film phototransistors and the majority of small molecular phototransistors,[6, 7, 34, 42, 48-55] as shown in Table 1. The fast response time in the current PTHPs deems it suitable for a high-speed switching device.

(insert Table 1 here)

2.3 The influence of mobility on the performances of phototransistors

The mobility of polymer semiconductors is important in terms of its efficiency for the processes of transporting carriers and collecting carriers of phototransistors. Low mobility limits the processes while high mobility promotes the processes. To investigate the effect of mobility on the photoresponse characterization of PBIBDF-BT PTHPTs, we fabricated

devices based on PBIBDF-BT thin-films spun at different spinning speeds. Previous works have revealed that the mobilities of polymer transistors were highly dependent upon the spinning speed during film formation process.[56, 57]

(insert Figure 5 and 6 here)

Figure 5 summarizes the carrier mobility obtained from the phototransistors in dark conditions at the saturation region as a function of spinning speeds. Interestingly, both the hole- and electron- mobility of PBIBDF-BT transistor show a monotonously increasing tendency as spinning speed increases. The devices spun at 6000 rpm display the highest hole mobility of 0.56 $cm^2V^{-1}s^{-1}$ with the average at 0.45 ± 0.02 $cm^2V^{-1}s^{-1}$ and the highest electron mobility of 0.15 $cm^2V^{-1}s^{-1}$ with the average at 0.12 ± 0.02 $cm^2V^{-1}s^{-1}$. The thin film morphological and microstructural properties of PBIBDF-BT were investigated using atomic force microscopy (AFM) in the tapping-mode. As shown in Figure 6, all samples prepared at different spin speeds present a fibrous texture. Our previous work has shown that the PBIBDF-BT molecules prefer to form fibrillar crystals with a dimension in the range of dozens of nanometers due to the strong intermolecular π-π interactions.[36] Therefore, the fibers observed in Figure 6 should display aggregations of nanofibrils of PBIBDF-BT. As the spin speed increases from 4000 rpm to 6000 rpm, the dimensions of the fibers clearly decrease, which could be ascribed to the necking effect of fibers caused by higher shearing force at higher spin speed. The higher shearing force can induce ordered packing in a film that may largely contribute to its high charge carrier mobility,[58-61] as shown in Figure 5. Moreover，the film thickness can also affect on the device performance. AFM was carried out to analyze the film thickness of PBIBDF-BT spun at different speeds. Figure S3a-c show the AFM image in the region near film and OTS-treated substrate. The vertical distance between film and substrate present the thickness of the films. As shown in Figure S3, the films become thinner with the increase of spin speed. And the thicknesses of the films spun at 4000 rpm, 5000 rpm, and 6000 rpm, are 83 ± 2 nm, 72 ± 2 nm, and 63 ± 2 nm, respectively. For devices with top contact configuration, the thinner semiconductor film might benefit for charge injection from source electrode to semiconducting layer, resulting in higher charge carrier mobility.

Therefore, both microstructures and film thickness would be the main reason for the enhanced performance with the increase of spin speed.

To evaluate the effect of mobility on photoresponse characteristics of PBIBDF-BT PTHPTs, the photoresponsity, on/off current ratios, and response speed of the device prepared at spinning speeds of 4000, 5000, and 6000 rpm were compared, as shown in Figure 7 and Table 2. As seen in Figure 7a, the maximum R calculated from hole- and electron- carriers transportation were 16.45, 49.61, 70.12 mAW^{-1} and 5.27, 18.07, 38.72 mAW^{-1} for devices spin-coated at 4000, 5000, and 6000 rpm, respectively. The on/off current ratios were measured to be 66, 238, and 1113 for P-type channel and 45, 231, and 597 for N-type channel at 4000, 5000, and 6000 rpm, respectively, as shown in Figure 7b; the figure clearly demonstrates the trend of on/off currents and photoresponsivity are increasing with increasing spinning speed.

(insert Figure 7 here)

(insert Table 2 here)

Table 2 summarizes the T_r and T_f of hole- and electron- carriers at different spinning speeds. Both T_r and T_f of devices spin-coated at 6000 rpm are less than 14 ms. As the spinning speed decreased, the response time increased. In summary, all properties of the PBIBDF-BT phototransistors including photoresponsivity， on/off current ratios, and response time displayed an improvement trend with the increase of spinning speed. These results indicate that the mobility of the organic semiconductor display an important role in determining the performance of phototransistor. A high mobility can enhance the performance of the polymer phototransistor.

3. Conclusions

A phototransistor based on D─A conjugated polymer semiconductor (PBIBDF-BT) is investigated herein. The phototransistor based on a polymer semiconductor exhibited both hole-carriers and electron-carriers transport and fast photoswitching speeds of less than 14 ms

to incident light. The response speed of PBIBDF-BT thin-film phototransistor is faster to light illumination relative to the majority of organic phototransistors. The devices demonstrated maximum values of photocurrent/dark current ratio of 4552 for hole-carriers transport and a P value of 1044 for electron-carriers transport. Furthermore, we discussed the influences of mobility on the response of the phototransistor to light illumination and proved that high mobility can enhance the performance of a phototransistor. All of the results herein should offer valuable information in the development of organic semiconductors in organic optoelectronic applications, especially in the use of D─A conjugated polymers.

4. Experimental section

4.1 Materials:

Chloroform (CF) and trichloro(octadecyl)silane (OTS) were purchased from Sigma-Aldrich Chemical Ltd. PBIBDF-BT was synthesized by our research group.

4.2 Measurements and Characterization:

The optical UV behavior of PBIBDF-BT was recorded on a Perkin Elmer model λ 20 UV-vis spectrophotometer. The morphologies of PBIBDF-T films were characterized with atomic force microscopy (AFM) (Digital Instruments Multimode). Electrical characterization of the PTFPTs under dark and illuminated conditions were measured by using a Keithley 4200-SCS semiconductor parametric. The light-emitting diode (LED) lamp (650 nm) was employed as the illumination source. The optical power was measured with a calibrate silicon photodiode. The photocurrent (I_{ph}) was calculated by subtracting the dark current (I_{dark}) form current under illumination. The field-effect mobility (μ_{FET}) and the threshold voltage (V_{TH}) in dark and illuminated conditions were estimated in the saturation regime (V_{DS} = -80 V) with the following equation: $I_{DS} = \mu_{FET}C_g(V_{GS}-V_{TH})^2W/2L$, where I_{DS} is the drain current, C_g is the capacitance of the gate-dielectric, and V_{GS} is the gate-source voltage.

4.3 Device Fabrication:

The PTFPTs were fabricated in a bottom-gate, top contact configuration. Heavily-doped silicon wafers (n-type, <0.004 Ω·cm) with thermally grown 300-nm-thick SiO_2 were used as substrates. The SiO_2/Si wafers were cleaned with pure water, pure alcohol, and pure acetone. The Si/SiO_2 wafers were then treated with trichloro(octadecyl)silane (OTS) by a normal vapor

deposition method. Hence OTS/SiO_2 and heavily-doped Si were utilized as the gate-dielectric and gate-electrode, respectively. A chloroform solution containing PBIBDF-BT polymer semiconductor (solution concentration, 5 mg/L) was dropped onto OTS/SiO_2/Si substrates and spin-coated at 4000, 5000, and 6000 rpm and the polymer films were subsequently annealed (175 °C) for 15 min in a nitrogen-filled glove box. Gold source/drain electrodes (30 nm) were thermally evaporated via a shadow mask onto the PBIBDF-BT thin-film layer. The source/drain patterns had a channel length (L) of 150 μm and a channel width (W) of 800 μm.

5. Acknowledgments

National Natural Science Foundation of China (Grand No. 21174036, 2120417, 51203039), Program for New Century Excellent Talents in University (Grant No.NCET-12-0839), and the Fundamental Research Funds for the Central Universities.

6. Notes and references

1. C. Wang, H. Dong, W. Hu, Y. Liu and D. Zhu, *Chem. Rev.*, 2012, **112**, 2208-2267.
2. B. Kang, H. Min, U. Seo, J. Lee, N. Park, K. Cho and H. S. Lee, *Adv. Mater.*, 2013, **25**, 4117-4122.
3. J. Mei, Y. Diao, A. L. Appleton, L. Fang and Z. Bao, *J. Am. Chem. Soc.*, 2013, **135**, 6724-6746.
4. X. Liu, Y. Guo, Y. Ma, H. Chen, Z. Mao, H. Wang, G. Yu and Y. Liu, *Adv. Mater.*, 2014, **26**, 3569-3569.
5. R. S. Ashraf, I. Meager, M. Nikolka, M. Kirkus, M. Planells, B. C. Schroeder, S. Holliday, M. Hurhangee, C. B. Nielsen, H. Sirringhaus and I. McCulloch, *J. Am. Chem. Soc.*, 2015, **137**, 1314-1321.
6. K.-J. Baeg, M. Binda, D. Natali, M. Caironi and Y.-Y. Noh, *Adv. Mater.*, 2013, **25**, 4267-4295.
7. H. Dong, H. Zhu, Q. Meng, X. Gong and W. Hu, *Chem. Soc. Rev.*, 2012, **41**, 1754-1808.
8. W. H. Lee, J. H. Cho and K. Cho, *J. Mater. Chem.*, 2010, **20**, 2549-2561.
9. H. E. A. Huitema, G. H. Gelinck, J. B. P. H. van der Putten, K. E. Kuijk, C. M. Hart, E. Cantatore, P. T. Herwig, A. J. J. M. van Breemen and D. M. de Leeuw, *Nature*, 2001, **414**, 599-599.
10. H. Sirringhaus, T. Kawase, R. H. Friend, T. Shimoda, M. Inbasekaran, W. Wu and E. P. Woo, *Science*, 2000, **290**, 2123-2126.
11. B. Crone, A. Dodabalapur, Y. Y. Lin, R. W. Filas, Z. Bao, A. LaDuca, R. Sarpeshkar, H. E. Katz and W. Li, *Nature*, 2000, **403**, 521-523.
12. P. Lin and F. Yan, *Adv. Mater.*, 2012, **24**, 34-51.
13. L. Ma, Z. Yi, S. Wang, Y. Liu and X. Zhan, *J. Mater. Chem. C*, 2015, **3**, 1942-1948.
14. Y. Liu, H. Wang, H. Dong, J. Tan, W. Hu and X. Zhan, *Macromolecules*, 2012, **45**, 1296-1302.
15. H. Dong, Z. Bo and W. Hu, *Macromol. Rapid Commun.*, 2011, **32**, 649-653.
16. G. Zhang, J. Guo, M. Zhu, P. Li, H. Lu, K. Cho and L. Qiu, *Polym. Chem.*, 2015, **6**, 2531-2540.
17. T. T. Steckler, P. Henriksson, S. Mollinger, A. Lundin, A. Salleo and M. R. Andersson, *J. Am. Chem. Soc.*, 2014, **136**, 1190-1193.
18. K. H. Hendriks, W. Li, M. M. Wienk and R. A. J. Janssen, *J. Am. Chem. Soc.*, 2014, **136**, 12130-12136.
19. M. Mas-Torrent and C. Rovira, *Chem. Rev.*, 2011, **111**, 4833-4856.
20. S. Günes, H. Neugebauer and N. S. Sariciftci, *Chem. Rev.*, 2007, **107**, 1324-1338.
21. M. Li, C. An, T. Marszalek, X. Guo, Y.-Z. Long, H. Yin, C. Gu, M. Baumgarten, W. Pisula and K. Müllen, *Chem. Mater.*, 2015, **27**, 2218−2223.
22. J. H. Park, E. H. Jung, J. W. Jung and W. H. Jo, *Adv. Mater.*, 2013, **25**, 2583-2588.
23. I. Kang, H.-J. Yun, D. S. Chung, S.-K. Kwon and Y.-H. Kim, *J. Am. Chem. Soc.*, 2013, **135**, 14896-14899.
24. G. Kim, S.-J. Kang, G. K. Dutta, Y.-K. Han, T. J. Shin, Y.-Y. Noh and C. Yang, *J. Am. Chem. Soc.*, 2014, **136**, 9477-9483.
25. T. W. Lee, D. H. Lee, J. Shin, M. J. Cho and D. H. Choi, *Polym. Chem.*, 2015, **6**, 1777-1785.
26. Z. Fei, P. Pattanasattayavong, Y. Han, B. C. Schroeder, F. Yan, R. J. Kline, T. D. Anthopoulos and M. Heeney, *J. Am. Chem. Soc.*, 2014, **136**, 15154-15157.
27. H.-J. Yun, H. H. Choi, S.-K. Kwon, Y.-H. Kim and K. Cho, *Chem. Mater.*, 2014, **26**, 3928-3937.
28. B. Sun, W. Hong, Z. Yan, H. Aziz and Y. Li, *Adv. Mater.*, 2014, **26**, 2636-2642.
29. H.-J. Yun, S.-J. Kang, Y. Xu, S. O. Kim, Y.-H. Kim, Y.-Y. Noh and S.-K. Kwon, *Adv. Mater.*, 2014, **26**,

7300-7307.

30. B. Sun, W. Hong, H. Aziz and Y. Li, *Polym. Chem.*, 2015, **6**, 938-945.
31. J. H. Park, H. S. Lee, S. Park, S.-W. Min, Y. Yi, C.-G. Cho, J. Han, T. W. Kim and S. Im, *Adv. Funct. Mater.*, 2014, **24**, 1109-1116.
32. L.-B. Luo, J.-J. Chen, M.-Z. Wang, H. Hu, C.-Y. Wu, Q. Li, L. Wang, J.-A. Huang and F.-X. Liang, *Adv. Funct. Mater.*, 2014, **24**, 2794-2800.
33. B. Mukherjee, M. Mukherjee, Y. Choi and S. Pyo, *J. Phys. Chem. C*, 2009, **113**, 18870-18873.
34. S. Dutta and K. S. Narayan, *Phys. Rev. B*, 2003, **68**, 125208.
35. T. D. Anthopoulos, *Appl. Phys. Lett.*, 2007, **91**, 113513.
36. T. Lei, J.-H. Dou, X.-Y. Cao, J.-Y. Wang and J. Pei, *J. Am. Chem. Soc.*, 2013, **135**, 12168-12171.
37. Z. Yan, B. Sun and Y. Li, *Chem. Commun.*, 2013, **49**, 3790-3792.
38. T. Lei, J.-H. Dou, X.-Y. Cao, J.-Y. Wang and J. Pei, *Adv. Mater.*, 2013, **25**, 6589-6593.
39. G. Zhang, P. Li, L. Tang, J. Ma, X. Wang, H. Lu, B. Kang, K. Cho and L. Qiu, *Chem. Commun.*, 2014, **50**, 3180-3183.
40. M. C. Hamilton, S. Martin and J. Kanicki, *IEEE Trans. Electron Devices*, 2004, **51**, 877-885.
41. L.-H. Zeng, M.-Z. Wang, H. Hu, B. Nie, Y.-Q. Yu, C.-Y. Wu, L. Wang, J.-G. Hu, C. Xie, F.-X. Liang and L.-B. Luo, *ACS Appl. Mat. Interfaces*, 2013, **5**, 9362-9366.
42. H. Dong, H. Li, E. Wang, H. Nakashima, K. Torimitsu and W. Hu, *J. Phys. Chem. C*, 2008, **112**, 19690-19693.
43. T. Pal, M. Arif and S. I. Khondaker, *Nanotechnology*, 2010, **21**, 325201.
44. L. Zhang, D. Yang, S. Yang and B. Zou, *Appl. Phys. A*, 2014, **116**, 1511-1516.
45. H. Li, Y. Wu, X. Wang, Q. Kong and H. Fu, *Chem. Commun.*, 2014, **50**, 11000-11003.
46. X. Wang, K. Wasapinyokul, W. De Tan, R. Rawcliffe, A. J. Campbell and D. D. C. Bradley, *J. Appl. Phys.*, 2010, **107**, 024509.
47. K. S. N. a. N. Kumar, *Appl. Phys. Lett.*, 2001, **79**, 1891-1893.
48. M. Y. Cho, S. J. Kim, Y. D. Han, D. H. Park, K. H. Kim, D. H. Choi and J. Joo, *Adv. Funct. Mater.*, 2008, **18**, 2905-2912.
49. S. Dutta and K. S. Narayan, *Adv. Mater.*, 2004, **16**, 2151-2155.
50. K. H. Kim, S. Y. Bae, Y. S. Kim, J. A. Hur, M. H. Hoang, T. W. Lee, M. J. Cho, Y. Kim, M. Kim, J.-I. Jin, S.-J. Kim, K. Lee, S. J. Lee and D. H. Choi, *Adv. Mater.*, 2011, **23**, 3095-3099.
51. J. G. Labram, P. H. Wöbkenberg, D. D. C. Bradley and T. D. Anthopoulos, *Org. Electron.*, 2010, **11**, 1250-1254.
52. X. Zhang, J. Jie, W. Zhang, C. Zhang, L. Luo, Z. He, X. Zhang, W. Zhang, C. Lee and S. Lee, *Adv. Mater.*, 2008, **20**, 2427-2432.
53. T. P. I. Saragi, R. Pudzich, T. Fuhrmann and J. Salbeck, *Appl. Phys. Lett.*, 2004, **84**, 2334-2336.
54. F. Yan, J. Li and S. M. Mok, *J. Appl. Phys.*, 2009, **106**, 074501.
55. B. Lucas, A. El Amrani, M. Chakaroun, B. Ratier, R. Antony and A. Moliton, *Thin Solid Films*, 2009, **517**, 6280-6282.
56. K. Kotsuki, H. Tanaka, S. Obata, S. Stauss, K. Terashima and K. Saiki, *Appl. Phys. Lett.*, 2014, **104**, 233306.
57. D. M. DeLongchamp, B. M. Vogel, Y. Jung, M. C. Gurau, C. A. Richter, O. A. Kirillov, J. Obrzut, D. A. Fischer, S. Sambasivan, L. J. Richter and E. K. Lin, *Chem. Mater.*, 2005, **17**, 5610-5612.
58. Y. Liu, Y. Liu and X. Zhan, *Macromol. Chem. Phys.*, 2011, **212**, 428-443.
59. Y. Liu, H. Dong, S. Jiang, G. Zhao, Q. Shi, J. Tan, L. Jiang, W. Hu and X. Zhan, *Chem. Mater.*,

2013, **25**, 2649-2655.

60. Y. Liu, H. Wang, H. Dong, L. Jiang, W. Hu and X. Zhan, *Small*, 2013, **9**, 294-299.

61. Y. Liu, Q. Shi, L. Ma, H. Dong, J. Tan, W. Hu and X. Zhan, *J. Mater. Chem. C*, 2014, **2**, 9505-9511.

Table and Figure Captions:

Table 1. Response speed of phototransistors based organic semiconductors.

Table 2. Photocurrent rise time and fall time of phototransistors formed at different spinning speeds.

Figure 1. (a) Chemical structure of PBIBDF-BT. (b) Schematic diagram of the polymer thin-film phototransistor. (c) UV-vis NIR absorption spectra of PBIBDF-BT in chloroform, in thin film and thin film annealed at 175 °C.

Figure 2. Linear and saturation regions of transfer characteristics of devices based on PBIBDF-BT under illumination compared with darkness, (a) V_{DS} = -10 V, (b) V_{DS} = 10 V, (c) V_{DS} = -80 V, and (d) V_{DS} = 80 V. Output characteristics of devices under illumination compared with darkness, (e) V_{GS} = -40 V and (f) V_{GS} = 40 V.

Figure 3. Photocurrent vs. time plot of PBIBDF-BT device at different intensities at the same applied bias of (a) V_{GS} = V_{DS} = -10 V, (b) V_{GS} = V_{DS} = 10 V. Time dependent photoresponse of the phototransistors measured by periodically turning on and off the light intensity (21.68 $mWcm^{-2}$) of a light source (650 nm), (c) V_{GS} =V_{DS} = -10 V, (d) V_{GS} = V_{DS} = 10 V. The time interval of switching the light on and off is 10 seconds.

Figure 4. Photocurrent rise time and fall time of the devices with different spinning speeds for (a) rise time of electron- and hole-carriers transport and (b) fall time of electron- and hole-transport.

Figure 5. Mobility values calculated from devices at three spinning speeds during the spin-coating process for (a) hole-carriers transport and (b) electron-carriers transport.

Figure 6. AFM images of the PBIBDF-BT thin-film morphologies by spin-coating on OTS/SiO_2/Si substrates at a spinning speed of (a) 4000 rpm, (b) 5000 rpm, and (c) 6000 rpm.

Figure 7. (a) The maximum values of photoresponsivity of devices spun at different spinning speeds. (b) The average values of on/off current ratios of devices spun at different spinning speeds.

Tables:

Table 1. Response speed of phototransistors based organic semiconductors.

Semiconductor	Structure (Dielectric)	Response speed	References
P3HT	BG/TC (PVA)	< 20 ms	34
TA-PPE	BG/TC (SiO_2, OTS)	< 10 s*	42
$F_{16}CuPc$	BG/TC (P4PMS)	10 ms	33
Pentacene	BG/TC (PMMA)	0.1 s	55
Spiro-DPSP	BG/BC (SiO_2, HMDS)	1.5 s	53
A-EHDTT	BG/TC (SiO_2, OTS)	~ 15 s	50
4(HPBT)-benzene	BG/BC (SiO_2)	< 1 s	48
Pentacene/$PC_{61}BM$	BG/BC (ODPA)	210 ms	51
MDMO-PPV:$PC_{61}BM$	BG/BC (SiO_2, HMDS)	~ 16 μs	35
P3HT:TiO_2	BG/BC (SiO_2)	~ 0.2 s	54
PBIBDF-BT	BG/TC (SiO_2, OTS)	~ 14 ms	Our work

* the value are estimated from the figures of response speed in corresponding references.

Table 1.

Table 2. Photocurrent rise time and fall time of phototransistors formed at different spinning speeds.

	4000 rpm		5000 rpm		6000 rpm	
	T_r	T_f	T_r	T_f	T_r	T_f
hole	~42 ms	~28 ms	~14 ms	~14 ms	~14 ms	~14 ms
electron	~28 ms	~14 ms	~14 ms	~28 ms	~14 ms	~14 ms

Table 2.

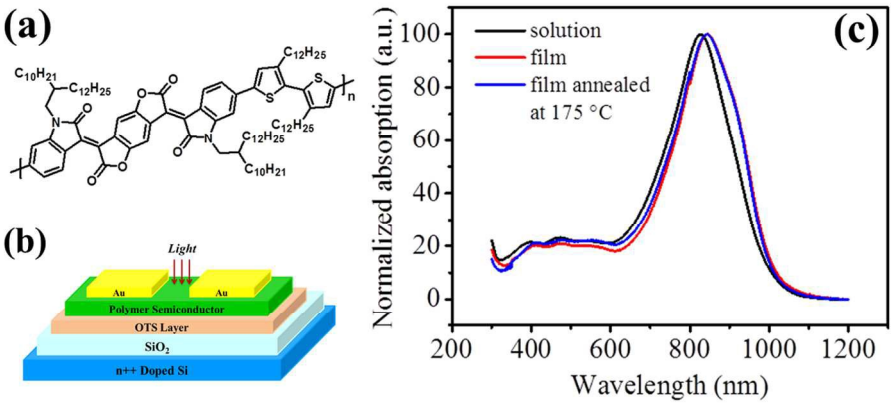

Figure 1.
395x177mm (96 x 96 DPI)

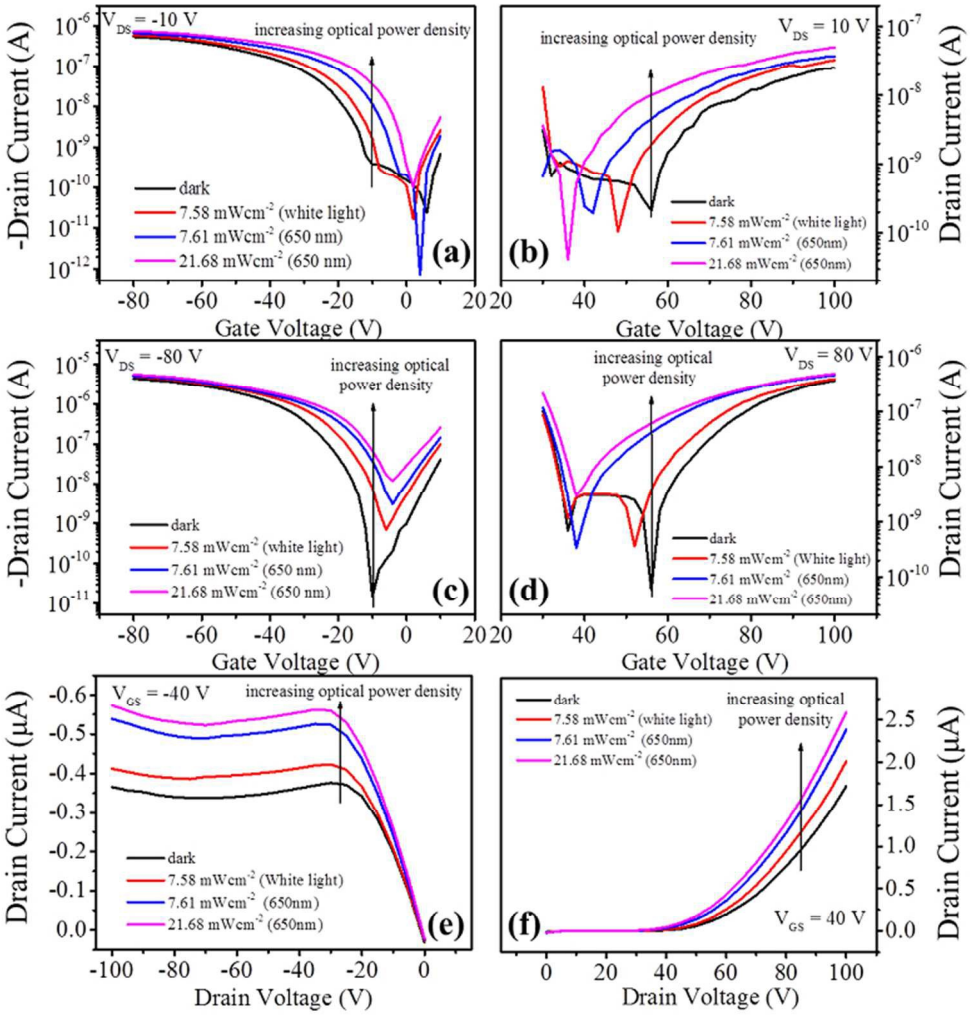

Figure 2.
211x223mm (96 x 96 DPI)

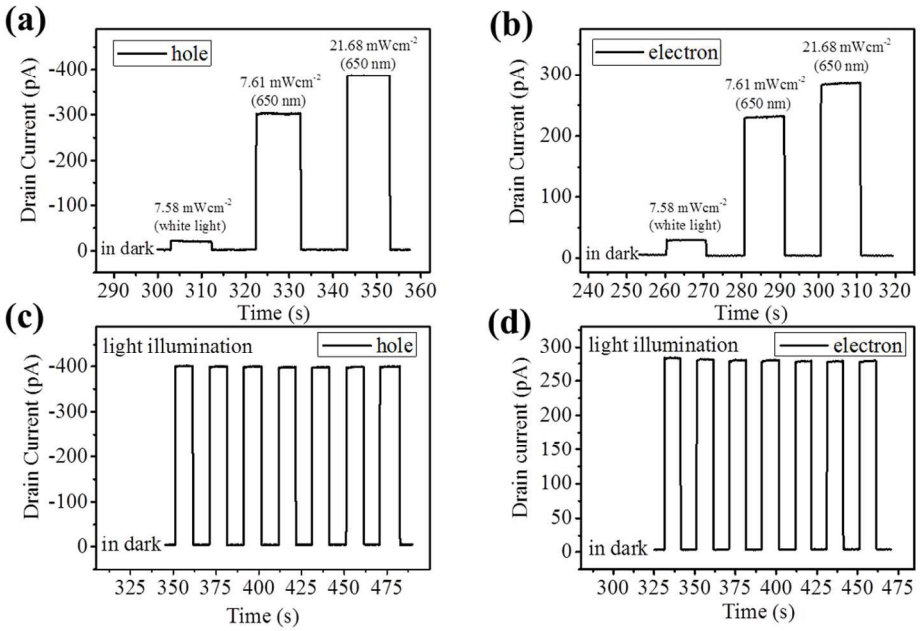

Figure 3.
341x220mm (96 x 96 DPI)

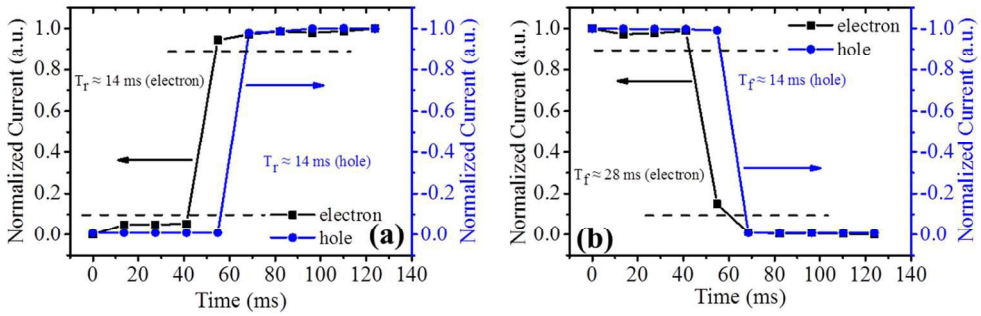

Figure 4.
332x116mm (96 x 96 DPI)

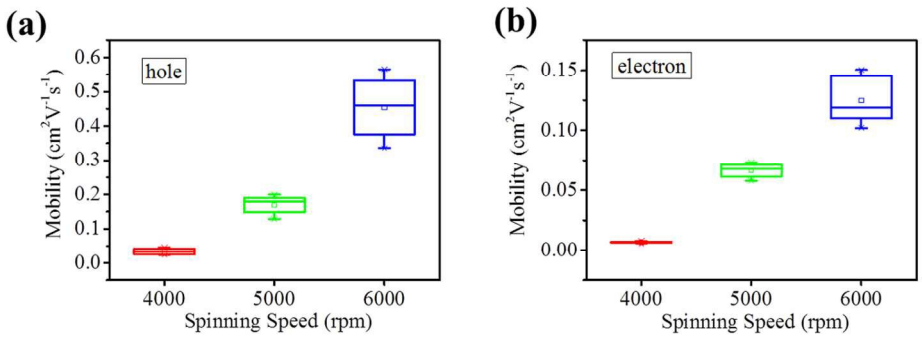

Figure 5.
345x121mm (96 x 96 DPI)

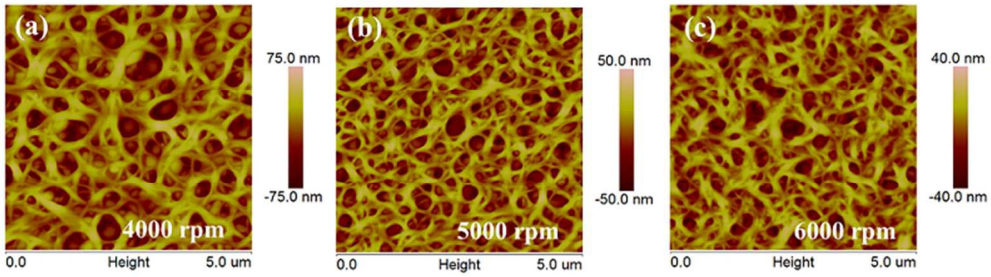

Figure 6.
211x58mm (96 x 96 DPI)

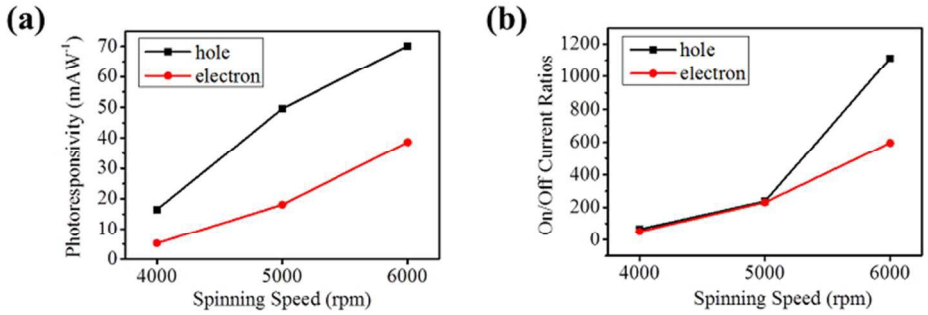

Figure 7.
211x69mm (96 x 96 DPI)

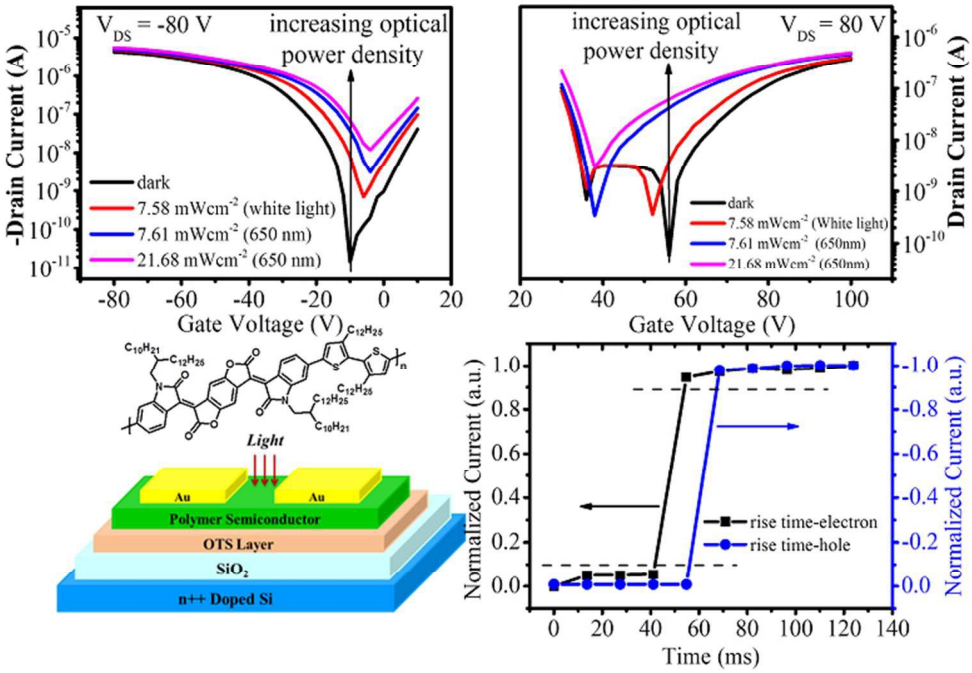

Graphical Abstract.
211x150mm (96 x 96 DPI)

A D─A polymer phototransistor shows both hole- and electron-carriers transport response to incident light with photoswitching speeds below 14 ms.